PERGAMON

International Journal of Solids and Structures 40 (2003) 5125–5138

INTERNATIONAL JOURNAL OF SOLIDS and STRUCTURES

www.elsevier.com/locate/ijsolstr

A coupled tire structure/acoustic cavity model

L.R. Molisani [a,*], R.A. Burdisso [a], Dimitri Tsihlas [b]

[a] *Vibration and Acoustics Laboratories, Department of Mechanical Engineering, Virginia Polytechnic Institute and State University, Office 12-B Randolph Hall, Blacksburg, VA 24061-0238, USA*

[b] *Michelin North America, Inc., Noise and Vibration Team, 515 Michelin Rd., Greenville, SC 29062-198, USA*

Received 3 September 2002; received in revised form 16 January 2003

Abstract

The dynamic characteristic of the tires is a key factor in the road-induced interior noise in passenger vehicles. The tire acoustic cavity is a very important factor in the tire dynamics and it must be considered in analyses. This paper describes a closed form analytical model for tire-wheel structures. In order to incorporate the dynamics of the cavity on the tire response, the tire acoustic-structure coupled problem is solved simultaneously. The tire is modeled as an annular cylindrical shell where only the outside shell is flexible, i.e. tire sidewalls and wheel are assumed rigid. From the analytical solution of the eigenproblems, both the tire structure and cavity acoustic responses are expanded in terms of their eigenfunctions. The main objective of the model is to have an efficient tool to investigate the physical coupling mechanisms between the acoustic cavity and the tire structure without the need of complicated numerical model such as finite elements. The result shows that the proposed model captures the main mechanisms of the effect of the tire air acoustic on the tire dynamics.

Keywords: Acoustic cavity resonances; Acoustic cavity–tire structure interaction

1. Introduction

The automotive industry is involved in a continuous endeavor to improve the noise and vibration characteristics of passenger vehicles. The reduction of interior noise is one of such efforts. Under road condition, the noise spectrum inside a passenger vehicle is dominated by peaks. In the low frequency range <400 Hz, the interior noise is mainly structural borne noise and many of the peaks are due to structural resonances, e.g. body, tire-wheel assembly, and so forth. In a road test, Sakata et al. (1990) showed that noise inside the vehicle compartment correlated very well to the forced measured at the spindle below 400 Hz, thus validating the structural borne nature of the low frequency noise. In this same work, Sakata et al. (1990) have also for the first time shown that the tire air cavity resonances shows up as two distinct narrow

* Corresponding author. Tel.: +1-540-231-2390; fax: +1-540-231-8836.
E-mail address: lmolisan@vt.edu (L.R. Molisani).

0020-7683/$ - see front matter © 2003 Elsevier Ltd. All rights reserved.
doi:10.1016/S0020-7683(03)00259-2

peaks in the 200–300 Hz band of the noise spectrum. The implication of this work is that the acoustic resonances results in a force applied to the vehicle's spindle, which in turns drives the vehicle interior acoustic field. Therefore, in recent years the tire air cavity acoustics has become a major feature of interior noise studies and of great concern to the industry.

Simple one-dimensional models have been used to predict the cavity resonance frequencies of the undeformed tire geometry by both Sakata et al. (1990) and Thompson (1995). The fundamental acoustic resonance frequency corresponds to a plane wave propagating around the cavity torus, i.e. circumference of tire equal to acoustic wavelength. In addition, some physical insight has also been gained into the understanding of the direction of the forces acting on the spindle due to these acoustics resonances, Thompson (1995). Finite element (FE) models of the acoustic cavity were also used to investigate the effect of the deformation resulting from the contact with the ground, Sakata et al. (1990) and Yamauchi and Akiyoshi (2002). The results from this study showed that the deformation of the tire destroyed the axis-symmetry of the cavity and resulted into two closed resonances.

For the case of structure borne noise, the most effective approach to reduce the noise is by modification of components in the structural path. Thus, it is common practice to develop large detailed computer models of the vehicle components using FE. Subsequently, the component models are integrated using substructuring techniques for analysis of the system. The tire model is one of such sub-structures. To this end, Clayton and Saint-Cyr (1998) numerically incorporated the dynamics of the tire acoustic cavity into an existing 130,000 degree-of-freedoms tire FE model. Clayton and Saint-Cyr (1998) modeled the tire cavity using also FE and three formulations of fluid-structure coupling were investigated. Pietrzyk (2001) also developed FE models of tires and validated them with experimental results obtained on a non-rotating tire. Yamauchi and Akiyoshi (2002) have used a detailed FE models to investigate potential noise control solution to the cavity acoustic resonances problem.

Here a simple and effective closed form analytical model of the tire including the effect of the cavity resonance is developed. This model offers some advantages over large numerical FE models. One of the main advantages of the proposed model is that it can be used to uncover the coupling mechanisms between the acoustic cavity and the tire structure. These mechanisms are not easily determined and sometimes hidden in large numerical models. Another advantage of having a simple model is that it is more efficient to investigate potential noise control devices. Finally, the model presented can also predict the effect of the cavity resonance on the spindle forces and thus potentially used in conjunction with body structure model for interior noise predictions. In order to incorporate the dynamics of the cavity, the tire acoustic-structure coupled problem is solved simultaneously.

2. Structural theory

For an analytical closed form analysis, the tire was modeled as two shells of revolution and two annular plates as shown in Fig. 1. In this model, the outer shell was assumed to be the only elastic component while the inner shell and the two annular side plates are considered rigid. The outer shell has thickness h, radius a, and the inner shell radius is b. The structure connecting the tire to the spindle is also considered rigid. The boundary conditions for the outer shell were assumed to be simply supported, i.e. shear diaphragm edge conditions. The system is also assumed to be stationary, i.e. no rotation. The external excitation is a point force acting normal to the shell.

The equations of motion used for the thin circular cylindrical shell follows the Donnell–Mushtari theory, Leissa (1993). The first step in the model of the tire structure is to solve for the eigenvalue problem of the self-adjoint Donnell–Mushtari operator. The displacement vector is defined as $\{u, v, w\}^{\mathrm{T}}$ where they are the axial (u), tangential (v), and radial (w) displacement components. For the simply supported cylindrical shell of finite length, L, the displacement vector is given as

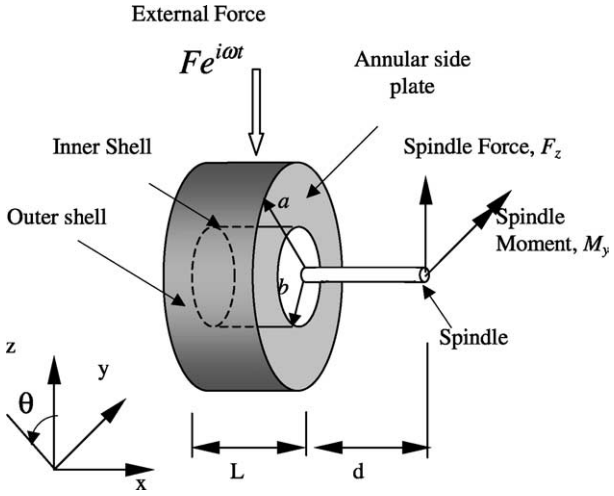

Fig. 1. Simplified tire model.

$$\{u_i\} = \begin{Bmatrix} u \\ v \\ w \end{Bmatrix} = \begin{Bmatrix} U\cos(\lambda_m)\cos(n\theta)\cos(\omega t) \\ V\sin(\lambda_m)\sin(n\theta)\cos(\omega t) \\ W\sin(\lambda_m)\cos(n\theta)\cos(\omega t) \end{Bmatrix} \quad n = 0, 1, 2, \ldots \quad m = 1, 2, 3, \ldots \tag{1}$$

where λ_m is

$$\lambda_m = m\pi\frac{a}{L} \quad \text{for } m = 1, 2, 3, \ldots$$

In Eq. (1), each pair of indices (m, n) defines the modal pattern, i.e. m defines the axial variation while n defines the azimuthal variation of the mode shape. The displacement vector in (1) defines the mode shapes. To find the mode natural frequencies, the Donnel–Mushtari operator is applied on the displacement as

$$\begin{bmatrix} a\frac{\partial^2}{\partial x^2} + \frac{(1-v^2)}{2}\frac{\partial^2}{\partial\theta^2} - \rho\frac{(1-v^2)a^2}{E}\frac{\partial^2}{\partial t^2} & \frac{(1+v)a}{2}\frac{\partial^2}{\partial x\partial\theta} & va\frac{\partial}{\partial x} \\ \frac{(1+v)a}{2}\frac{\partial^2}{\partial x\partial\theta} & \frac{\partial^2}{\partial\theta^2} + \frac{(1-v^2)a}{2}\frac{\partial^2}{\partial x^2} - \rho\frac{(1-v^2)a^2}{E}\frac{\partial^2}{\partial t^2} & \frac{\partial}{\partial\theta} \\ va\frac{\partial}{\partial x} & \frac{\partial}{\partial\theta} & 1 + K\nabla^4 + \rho\frac{(1-v^2)a^2}{E}\frac{\partial^2}{\partial t^2} \end{bmatrix} \cdot \begin{Bmatrix} u \\ v \\ w \end{Bmatrix} = \begin{Bmatrix} 0 \\ 0 \\ 0 \end{Bmatrix} \tag{2}$$

where ∇^2 is the Laplace's operator, $\nabla^4 \equiv \nabla^2\nabla^2$, and K is the non-dimensional thickness parameter defined by $K = h^2/12a^2$. The material properties are $E =$ Young's modulus, $\rho =$ density, and $v =$ Poison ratio of the tire. Replacing (1) into (2) leads to

$$\begin{bmatrix} -\lambda_m^2 - \frac{(1-v^2)}{2}n^2 + \Omega^2 & \frac{(1+v)}{2}n\lambda_m & v\lambda_m \\ \frac{(1+v)}{2}n\lambda_m & (1-v)\lambda_m^2 - n^2 + \Omega^2 & -n \\ -v\lambda_m & n & 1 + K(\lambda_m^2 + n^2)^2 - \Omega^2 \end{bmatrix} \cdot \begin{Bmatrix} U \\ V \\ W \end{Bmatrix} = \begin{Bmatrix} 0 \\ 0 \\ 0 \end{Bmatrix} \tag{3}$$

where Ω is called normalized frequency given as

$$\Omega = \sqrt{\frac{\rho(1-v^2)}{E}}a\omega \tag{4}$$

The "in-vacuum" eigenvalue problem in (4) will yield the shell natural frequencies and mode shapes. For each pair (m,n) defining a response pattern, the eigenvalue problem results in three natural frequencies which define three modes. In general, these modes are characterized by the dominance of one of the displacement vector component, i.e. longitudinally, tangentially, and radially dominated modes. The eigenvalues and eigenvectors are

$$\Omega_{mnj} \quad \text{and} \quad \begin{Bmatrix} U_{mn}^{(j)} \\ V_{mn}^{(j)} \\ W_{mn}^{(j)} \end{Bmatrix} \quad \text{for } (m,n) \quad j = 1,2,3 \tag{5}$$

By replacing the eigenvector from (5) into (1) leads to the eigenfunctions (or mode shapes)

$$\{\Phi_{mnj}\} = \begin{Bmatrix} U_{mn}^{(j)} \cos(n\theta)\cos\left(\lambda_m \frac{x}{a}\right) \\ V_{mn}^{(j)} \sin(n\theta)\sin\left(\lambda_m \frac{x}{a}\right) \\ W_{mn}^{(j)} \cos(n\theta)\sin\left(\lambda_m \frac{x}{a}\right) \end{Bmatrix} \tag{6}$$

Characteristic radial modal patterns for the circular cylindrical shells supported at both ends by "shear diaphragms", are shown in Fig. 2.

Fig. 2. Nodal patterns for circular cylindrical shells.

For the "in-vacuum" forced response, i.e. without the tire acoustic coupling, the differential equation of motion is now given by

$$\left([L_c] - \Omega^2[I]\right)\begin{Bmatrix} u \\ v \\ w \end{Bmatrix} = \begin{Bmatrix} 0 \\ 0 \\ f_w \end{Bmatrix} \tag{7}$$

where L_c is the shell differential operator defined in (2) and the external force is applied only in the radial direction. The response is expressed in terms of a linear combination of the modes as

$$\begin{Bmatrix} u \\ v \\ w \end{Bmatrix} = \sum_m \sum_n [\Phi_{mn}] \begin{Bmatrix} A_{mn1} \\ A_{mn2} \\ A_{mn3} \end{Bmatrix} \tag{8}$$

where A_{mnj} is the modal amplitudes of the (m, n, j) mode and $[\Phi_{mn}]$ is the 3×3 modal matrix for the modes defined by the pattern (m, n). To solve for the modal amplitudes Eq. (8) is pre-multiplied by the transpose of the modal matrix and integrated over the surface of the cylinder. Thus, the modal amplitudes are obtained from the following uncoupled system of equations,

$$\begin{bmatrix} K_{mn1} - \Omega^2 M_{mn1} & 0 & 0 \\ 0 & K_{mn2} - \Omega^2 M_{mn2} & 0 \\ 0 & 0 & K_{mn3} - \Omega^2 M_{mn3} \end{bmatrix} \cdot \begin{Bmatrix} A_{mn1} \\ A_{mn2} \\ A_{mn3} \end{Bmatrix} = \begin{Bmatrix} f_{mn1} \\ f_{mn2} \\ f_{mn3} \end{Bmatrix} \tag{9}$$

3. Acoustic theory

To account for the effect of the tire acoustic cavity response in the structural response, the acoustic mode shapes and natural frequencies are first computed for the annular cavity assuming rigid boundary conditions (Fig. 3).

The equation of motion for the acoustic cavity is given as

$$\nabla^2 \Psi = \frac{1}{c^2} \frac{\mathrm{d}^2 \Psi}{\mathrm{d}t^2} \tag{10}$$

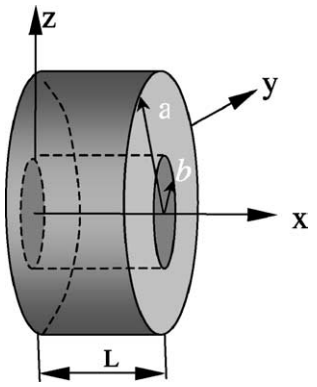

Fig. 3. Finite cylindrical cavity.

with

$$\Psi(r,\theta,x,t) = \Psi(r,\theta,x)\mathrm{e}^{\mathrm{i}\omega t} \tag{11}$$

Eq. (10) reduces to the Helmholtz equation

$$\nabla^2\Psi + k^2\Psi = 0 \tag{12}$$

where

$$k = \frac{\omega}{c} \tag{13}$$

and

$$\nabla^2(\cdot) + k^2(\cdot) \tag{14}$$

are the free field wave number and the Helmholtz self adjoin operator.

The rigid wall boundary conditions are defined as

$$\left(\frac{\mathrm{d}\Psi}{\mathrm{d}x}\right)_{x=0} = \left(\frac{\mathrm{d}\Psi}{\mathrm{d}x}\right)_{x=L} = \left(\frac{\mathrm{d}\Psi}{\mathrm{d}r}\right)_{r=a} = \left(\frac{\mathrm{d}\Psi}{\mathrm{d}r}\right)_{r=b} = 0 \tag{15}$$

The acoustic natural frequency, Blevins (1995), is then

$$\omega_{lqp} = c\sqrt{\left(\frac{p\pi}{a-b}\right)^2 + \left(\frac{2l}{a+b}\right)^2 + \left(\frac{q\pi}{L}\right)^2} \quad \text{with } b > 0.5a \tag{16}$$

and the mode acoustic shape is given by

$$\Psi_{lqp}(r,\theta,x) = \rho c^2 G_{pl}(r)\cos(p\theta)\cos(k_{xq}x) \quad \text{with } q,p,l = 0,1,2,\ldots \tag{17}$$

where

$$G_{pl}(r) = Y_p'(k_{pl})J_p\left(k_{pl}\frac{r}{a}\right) - J_p'(k_{pl})Y_p\left(k_{pl}\frac{r}{a}\right) \tag{18}$$

where J_p is the Bessel's function of first kind and Y_p is the Bessel's function of second kind. Orthogonality conditions of the acoustic modes leads to the normalization factor, Λ_{lqp}.

$$\int_0^{2\pi}\int_0^L\int_b^a \Psi_{lqp}(r,x,\theta)\Psi_{rso}(r,x,\theta)r\,\mathrm{d}r\,\mathrm{d}x\,\mathrm{d}\theta = \Lambda_{lqp}\delta_{lr}\delta_{qs}\delta_{po} \tag{19}$$

Fig. 4 illustrates a few acoustic modes shapes defined by the indices (l,q,p).

3.1. Coupled structural-acoustic problem

The cavity–structure interaction problem was solved knowing the "in vacuum" structure eigen-properties (mode shapes $\Phi_{mn}(x,\theta)$ and natural frequencies) and the interior acoustic eigen-properties (mode shape $\Psi_{lqp}(r,x,\theta)$ and natural frequencies), Fahy (2000). The pressure, i.e. fluid loading, is then expressed in terms of the velocity response of the tire. Fig. 5 illustrates the problem of a structure and the acoustic interior. It is important to remark that the description of the cavity-structural problem is quite complex due to the six indices required to describe the structural and acoustic modes. Here a brief description of the coupled problem will be presented for a general understanding of the solution approach.

The approach to solve the coupled problem is to include in the equation of motion of the tire the force due to the interior pressure. However, the fluid forces depend on the velocity response of the structure which leads to the fluid feedback problem depicted in Fig. 6.

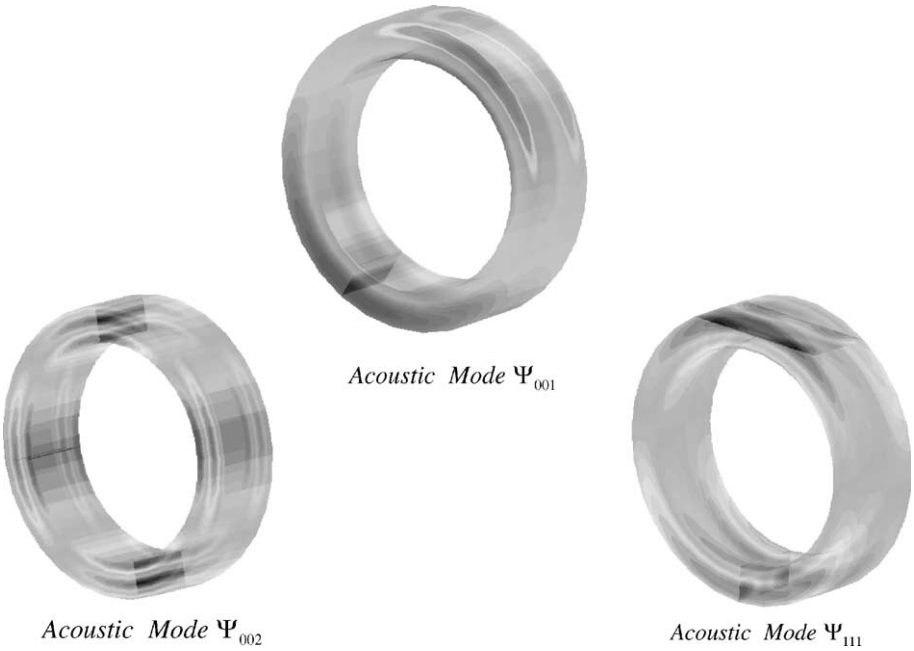

Fig. 4. Acoustics modes shapes Ψ_{lqp}.

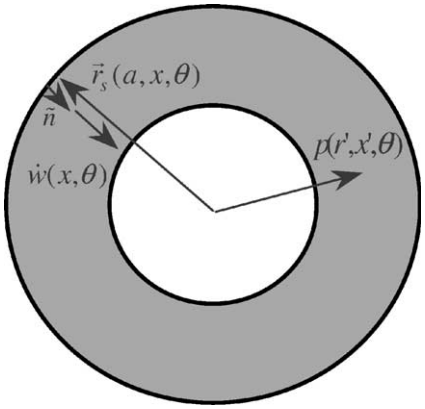

Fig. 5. Structure radiating into an enclosed volume.

The equation of motion of the system including the fluid loading is written as

$$\left\{[L_c] - \Omega^2[I]\right\} \cdot \begin{Bmatrix} u \\ v \\ w \end{Bmatrix} = \begin{Bmatrix} 0 \\ 0 \\ f_w \end{Bmatrix} - \begin{Bmatrix} 0 \\ 0 \\ p(a,x',\theta') \end{Bmatrix} \tag{20}$$

where the last vector in (20) represents the acoustic pressure acting on the tire. The acoustic pressure, $p(a,x',\theta')$, on the tire structure is given by

$$p(a,x',\theta') = \int_0^L \int_0^{2\pi} \mathrm{i}\omega\rho\dot{w}(x,\theta)G(a,x,\theta|a,x',\theta')a\,\mathrm{d}\theta\,\mathrm{d}x \tag{21}$$

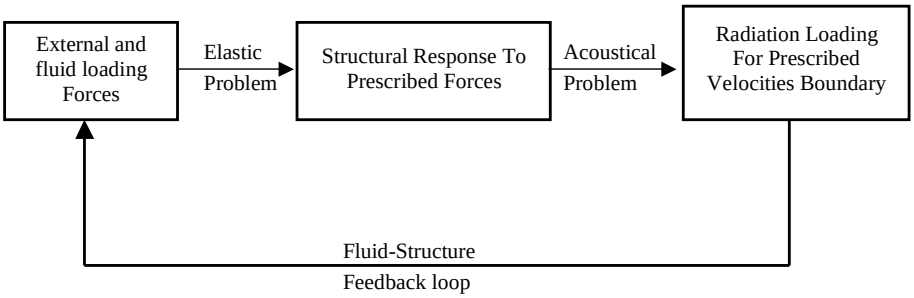

Fig. 6. Dynamic interaction between the structure and the fluid.

where $\dot{w}(x,\theta)$ is the radial component of the shell velocity response and $G(r,x,\theta|r',x',\theta')$ is the Green's function defined by

$$G(r,x,\theta|r',x',\theta') = \sum_{l}^{L}\sum_{q}^{Q}\sum_{p}^{P}\frac{\Psi_{lqp}(r,x,\theta)\Psi_{lqp}(r',x',\theta')}{\Lambda_{lqp}(k_{lqp}^2-k^2)} \tag{22}$$

where (p,q,l) represents an acoustic mode, and the integral of the product of two acoustic modes over the volume of the cavity, V, defines the mode normalization factor, Λ_{lqp}. The solution of the coupled problem is again obtained by expanding the structural response in term of the "in vacuum" modes as

$$\begin{Bmatrix} u \\ v \\ w \end{Bmatrix} = \sum_{m}^{M}\sum_{n}^{N}[\Phi_{mn}]\cdot\begin{Bmatrix} A_{mn1} \\ A_{mn2} \\ A_{mn3} \end{Bmatrix} \tag{23}$$

where A_{mnj} are now as the structural modal amplitudes including the fluid loading. Then, replacing (23) into (20), it gives

$$\left\{[L_c]-\Omega^2[I]\right\}\sum_{m}^{M}\sum_{n}^{N}[\Phi_{mn}]\begin{Bmatrix} A_{mn1} \\ A_{mn2} \\ A_{mn3} \end{Bmatrix} = \begin{Bmatrix} f_u \\ f_v \\ f_w \end{Bmatrix} - \begin{Bmatrix} 0 \\ 0 \\ p(a,x',\theta') \end{Bmatrix} \tag{24}$$

Once again this equation is pre-multiplied by the transpose of the modal matrix and integrated over the surface of the structure as

$$\begin{aligned}&\int_0^L\int_0^{2\pi}[\Phi_{rs}]^{\mathrm{T}}\left\{[L_c]-[\Omega]^2[I]\right\}[\Phi_{mn}]\begin{Bmatrix} A_{mn1} \\ A_{mn2} \\ A_{mn3} \end{Bmatrix} a\,\mathrm{d}\theta\,\mathrm{d}x \\ &\quad=\int_0^L\int_0^{2\pi}[\Phi_{rs}]^{\mathrm{T}}\left\{\begin{Bmatrix} f_u \\ f_v \\ f_w \end{Bmatrix} - \begin{Bmatrix} 0 \\ 0 \\ p(a,x',\theta') \end{Bmatrix}\right\} a\,\mathrm{d}\theta\,\mathrm{d}x\end{aligned} \tag{25}$$

The acoustic pressure acting on the surface of the structure $p(a,x',\theta')$ is obtained from (20) where the radial velocity component is replaced in terms of the structural modes and the modal amplitudes

$$p(a,x',\theta') = \int_0^L\int_0^{2\pi}\mathrm{i}\omega\rho_A\sum_{m}^{M}\sum_{n}^{N}\mathrm{i}\omega A_{mn}\Phi_{mn}\cdot\sum_{l}^{L}\sum_{q}^{Q}\sum_{p}^{P}\frac{\Psi_{lqp}(a,x,\theta)\Psi_{lqp}(a,x',\theta')}{\Lambda_{lqp}(k_{lqp}^2-k^2)}a\,\mathrm{d}\theta\,\mathrm{d}x \tag{26}$$

Since the only velocity component of the structural response that couples with the cavity is the radial one, in (26) only the radial modes are included in computing $p(a,x',\theta')$ in (26). Another implication of this assumption is that the acoustic cavity will affect on the radial structural modes. Replacing (26) into (25) and solving the integrals explicitly in terms of the unknown modal amplitudes of the radial modes, the following coupled system of equations results

$$\{[K]-\Omega^2[M]\}\cdot\{A_{mn}\}=\{f_{mn}\}-\Omega^2[\alpha]\cdot\{A_{mn}\} \tag{27}$$

where $[K]$ and $[M]$ are diagonal matrices and their elements represents the modal stiffness and mass of the radial modes; $\{A_{mn}\}$ is the vector of modal amplitudes; $\{f_{mn}\}$ is the vector of modal forces; and $[\alpha]$ is the fluid coupling matrix. The coefficients α_{mn} of this matrix are given by the product of the surface integrals as

$$\alpha_{mn}=\frac{\int_0^L\int_0^{2\pi}\Phi_{mn}(x,\theta)\Psi_{lqp}(a,x,\theta)a\,\mathrm{d}\theta\,\mathrm{d}x\int_0^L\int_0^{2\pi}\Phi_{mn}(x',\theta')\Psi_{lqp}(a,x',\theta')a\,\mathrm{d}\theta'\mathrm{d}x'}{\Lambda_{lqp}(k_{lqp}^2-k^2)} \tag{28}$$

The coefficient in (28) represents the effect of the (l,q,p) acoustic mode on the (m,n) structural radial mode. One of the advantage of the model develop here is that the interaction of the acoustic and structural modes can be easily determine by inspection of the coefficients in (28). If the coefficient α_{mn} vanishes implies that the (l,q,p) acoustic does not affect the (m,n) structural mode. This implies that acoustic and structural modes that have the same azimuth variation will be coupled. In addition, inspection of the integral in (28) will show the effect of the variation of the acoustic and structural modes on the coupling. The effect is illustrated in Table 1. In this table, it is shown the coupling of the (0,0,1) acoustic mode with the (1,1), (2,1), and (3,1) structural modes.

The modal amplitudes for the radial modes are obtained from Eq. (27), and the structural response is then obtained from (23) and then the acoustic response is computed using (26). The resulting spindle force

Table 1
Description of the effect of axial variation on the coupling between structural and acoustic modes of same azimuth variation

Acoustic $(l(r),q(x),p(\theta))$	Structural $(m(x),n(\theta))$		
		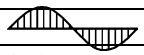	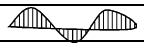
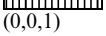	(1,1)	(2,1)	(3,1)
(0,0,1)	Coupling	No coupling	Coupling

Table 2
Index and frequencies associated to the structural modes shapes

Structure natural frequencies			
$m(x)$	$n(\theta)$	j	f_{mnj} (Hz)
1	1	1	228
1	1	2	785
1	1	3	1328
2	1	1	517.9
2	1	2	1555
2	1	3	2629
3	1	1	1090
3	1	2	2328
3	1	3	3937

F_z and moment M_y shown in Fig. 1 are also computed in the model. For the sake of brevity, this derivation is not presented here but it can be found in the work by Molisani and Burdisso (2000).

4. Numerical example

The numerical example consists of a tire with 0.2 m outer radius, 0.15 m inner radius, 0.01 m thickness, and 0.1 m width. Thus, the numerical example represents a 100/50R12 tire. The material properties used are

Table 3
Index and frequencies associated to the acoustic modes shapes

Acoustic natural frequencies			
$l(r)$	$q(x)$	$p(\theta)$	$f_{\ell qp}$ (Hz)
0	0	0	0
0	0	1	281.9
1	0	0	1715
1	0	1	1737
1	0	2	1804
2	0	0	3430

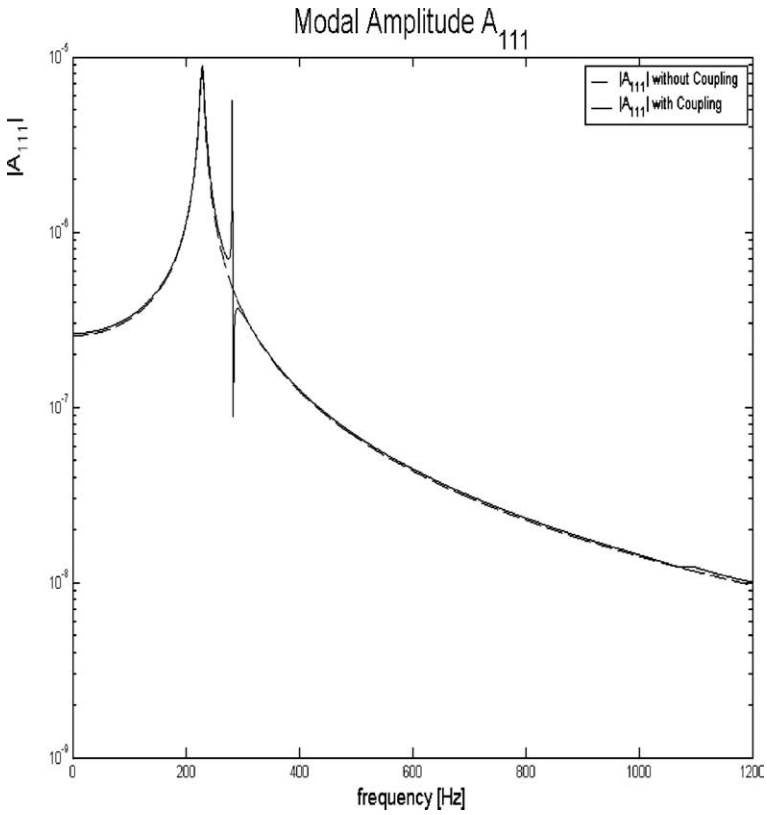

Fig. 7. Radial modal amplitude A_{111} with coupling and without coupling.

$E = 75 \times 10^6$ N/m^2, $\rho = 1200$ kg/m^3, and $v = 0.3$ ($\widehat{E} = E(1 + i\eta)$ with the loss factor $\eta = 0.03$). The air speed of sound is $c = 343$ m/s and the air density is $\rho = 1.2$ kg/m^3. The computed structural and acoustic resonance frequencies are presented in Tables 2 and 3, respectively. In Table 2, the j (1, 2, or 3) index indicates the dominant displacement component of the mode. The $j = 1$ index indicates radial dominated modes. Thus, the fundament structural is the radial (1,1) mode shown Fig. 2. On the other hand, the fundamental acoustic mode is the (0,0,1) mode shown in Fig. 4 with a natural frequency of 281.9 Hz. The commonly used approximation of assuming the length of the torus to be equal to the wavelength to predict the acoustic fundamental frequency yields 311 Hz, i.e. $c/[\pi(a + b)]$, which results in a $\sim$10% error (Sakata et al., 1990). In the frequency range of interest, only the (0,0,1) acoustic mode can couple with the (1,1) and (3,1) structural modes.

The "in-vacuum" and coupled responses were computed over the 0–1250 Hz range. The (1,1), (2,1), and (3,1) tire radial modes and the (0,0,1) acoustic mode are present in the response. Figs. 7 and 8 show the modal amplitudes for the (1,1) and (3,1) radial structural modes with (solid lines) and without (dashed lines) acoustic coupling respectively. It is clear in these figures that the effect of the tire acoustic cavity modes in the structural response is significant even though the acoustic resonance is not very close to the structural resonance. The modal responses for acoustic resonant frequencies are similar in magnitude as the response for the structural resonant frequencies. It is also interesting to note that the relatively high damping of the tire structure does not damp out the energy in the acoustic resonance. Fig. 8 also clearly reveals the

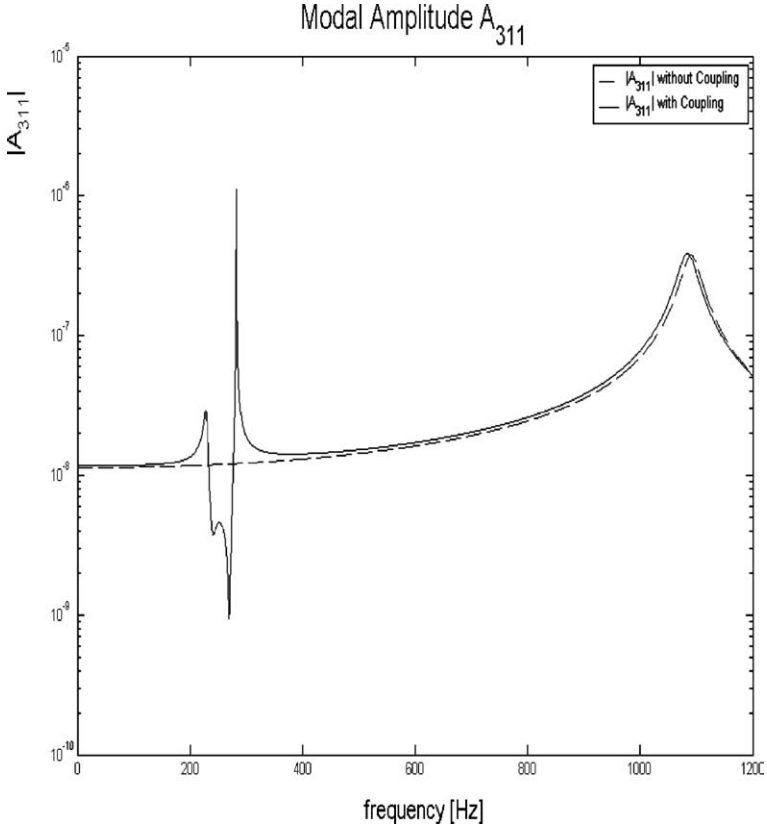

Fig. 8. Radial modal amplitude A_{311} with coupling and without coupling.

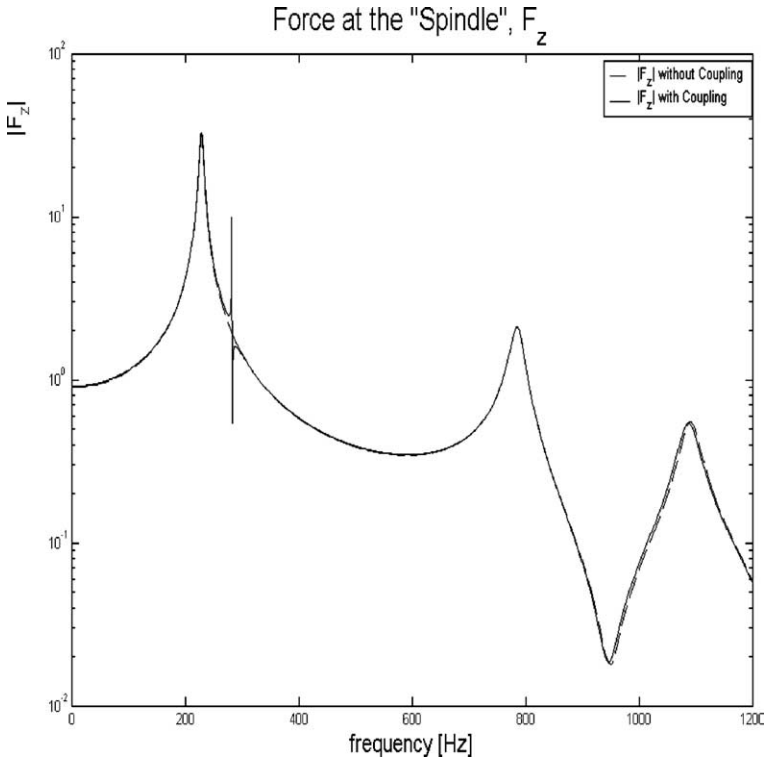

Fig. 9. Spindle force F_z with and without coupling.

coupling of the (1,1) and (3,1) mode introduced by the acoustic cavity (0,0,1) mode, i.e. the (1,1) mode is easily identified in the response of the (3,1) mode.

The resultant force and moment at the spindle were also computed using the approach developed by Molisani and Burdisso (2000). Figs. 9 and 10 show the spindle force and moment with and without acoustic coupling, respectively. Again they show that the internal acoustic cavity resonance effects are important and thus they should be accounted for in the prediction of vehicle interior noise. The results from this simple analytical model show qualitatively similar trends as experimental observation.

The model allows to clearly identifying the coupling mechanisms between the structural and acoustic modes. In addition, the results show that the acoustic cavity resonances have a significant effect on the response of the system, i.e. the cavity resonances results in important forces and moments at the spindle, which are the source of noise in the vehicle interior.

5. Conclusions

A simplified model of a tire including the dynamics of the acoustic cavity has been developed. The model was used to quantify the effect of the cavity resonances on the tire response as well as the transmitted force and moment at the spindle. The results clearly show that the acoustic resonance is important and needs to be included in the analysis. The model also shows that the relative high damping of the tire structure is not

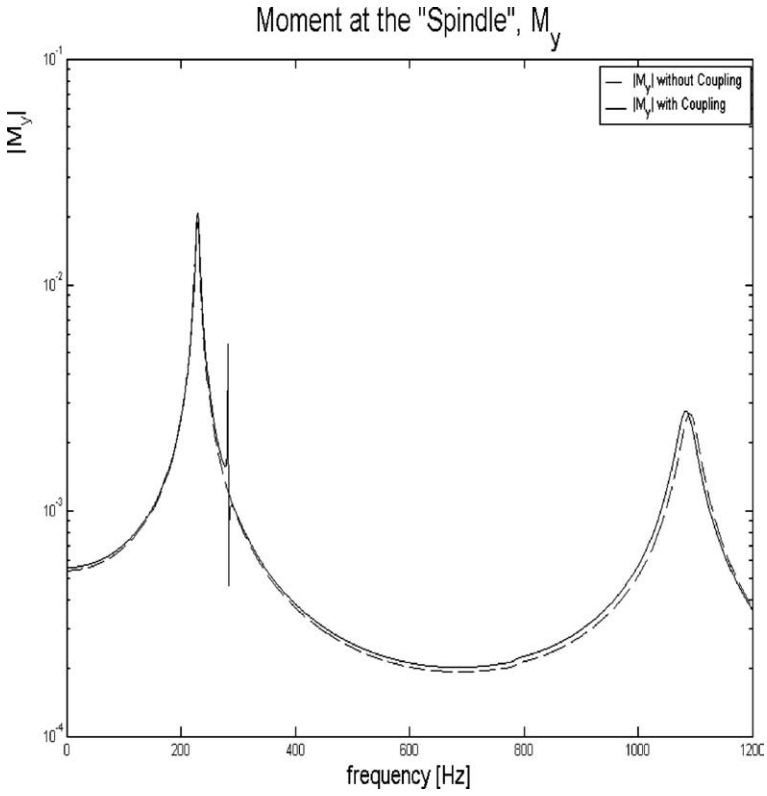

Fig. 10. Spindle moment M_y with and without coupling.

effective in damping out the energy in the acoustic resonance. The model also allows to gain insight into the coupling mechanisms between the acoustic and structural resonances.

Acknowledgement

This work for financially supported by Michelin North America, Inc. which is greatly appreciated.

References

Blevins, R., 1995. Formulas for Natural Frequency and Mode Shape. Krieger Publishing Company.

Clayton, W., Saint-Cyr, R., 1998. Incorporation of the tire air cavity resonance into the modal tire model. In: International Modal Analysis Conference IMAC XVI, 2–5 February, Santa Barbara, CA.

Fahy, F., 2000. Sound and Structural Vibration. Academic Press.

Leissa, A., 1993. Vibration of Shells. Acoustical Society of America.

Molisani, L., Burdisso, R., 2000. Modeling of the tire acoustic cavity and the effect on vehicle interior noise. In: Virginia Tech Final Report, Blacksburg, VA.

Pietrzyk, A., 2001. Prediction of the dynamic response of a tire. In: The 2001 International Congress and Exhibition on Noise Control Engineering INTER-NOISE 2001, 27–30 August, The Hague, The Netherlands.

Sakata, T., Morimura, H., Ide, H., 1990. Effect of tire cavity resonance on vehicle road noise. Tire Science and Technology 18, 68–79.
Thompson, J., 1995. Plane wave resonance in the air cavity as a vehicle interior noise source. Tire Science and Technology 23, 2–10.
Yamauchi, H., Akiyoshi, Y., 2002. Theoretical Analysis of Tire Acoustic Cavity Noise and Proposal of Improvement Technique, vol. 23. Society of Automotive Engineering of Japan. pp. 89–94.